Med Biol Eng Comput (2013) 51:153–164
DOI 10.1007/s11517-012-0980-y

ORIGINAL ARTICLE

A classification scheme for ventricular arrhythmias using wavelets analysis

K. Balasundaram · S. Masse · K. Nair · K. Umapathy

Received: 16 November 2011 / Accepted: 15 October 2012 / Published online: 7 November 2012

Abstract Identification and classification of ventricular arrhythmias such as rhythmic ventricular tachycardia (VT) and disorganized ventricular fibrillation (VF) are vital tasks in guiding implantable devices to deliver appropriate therapy in preventing sudden cardiac deaths. Recent studies have shown VF can exhibit strong regional organizations, which makes the overlap zone between the fast paced rhythmic VT and VF even more ambiguous. Considering that implantable cardioverter-defibrillator (ICD) are primarily rate dependent detectors of arrhythmias and that there may be patients who suffer from arrhythmias that fall in the overlap zone, it is essential to identify the degree of affinity of the arrhythmia toward VT or organized/disorganized VF. The method proposed in this work better categorizes the overlap zone using Wavelet analysis of surface ECGs. Sixty-three surface ECG signal segments from the MIT-BIH database were used to classify between VT, organized VF (OVF), and disorganized VF (DVF). A two-level binary classifier was used to first extract VT with an overall accuracy of 93.7 % and then the separation between OVF and DVF with an accuracy of 80.0 %. The proposed approach could assist clinicians to provide optimal therapeutic solutions for patients in the overlap zone of VT and VF.

Keywords Ventricular arrhythmia · Wavelet analysis · Singular value decomposition · Feature extraction · Pattern classification

K. Balasundaram · K. Umapathy (✉)
Department of Electrical and Computer Engineering, Ryerson University, Toronto, Canada
e-mail: karthi@ee.ryerson.ca

K. Balasundaram
e-mail: kbalasun@rnet.ryerson.ca

S. Masse · K. Nair
The Hull Family Cardiac Fibrillation Management Lab, Toronto General Hospital Toronto, Toronto, Canada
e-mail: stephane.masse@uhn.on.ca

K. Nair
e-mail: krishnakumar.nair@uhn.on.ca

1 Introduction

The two most significant ventricular arrhythmias are ventricular tachycardia (VT) and ventricular fibrillation (VF). VT is generally an organized arrhythmia. On the other hand, VF is a fundamentally chaotic, disorganized, abnormal and fast heart rhythm. Long-term therapy options for VT include anti-arrhythmic medications, ablation and implantable cardioverter-defibrillators (ICD). VF is nearly always an emergency, given its life-threatening nature. The only effective long-term option for VF is an ICD. The differentiation of these two arrhythmias is of immense clinical significance because of the difference in prognosis, immediate and long-term management.

There are programmed algorithms within the ICD that detect and act according to the type of arrhythmia. The algorithm usually selects between pacing maneuvers or shocking a patient depending on if the arrhythmia is VT or VF, respectively [50]. ICDs initially attempt to treat VT with overdrive pacing maneuvers or "painless therapy", failing which shocks are resorted to. For VF, all device companies have shock as the primary treatment option. Some device companies [47, 48] provide pacing while the ICD is charging prior to shocking in an attempt to provide treatment for those patients with fast VT. Though ICDs have helped patients for a few decades, if amenable, long-term solutions via ablation strategies are always preferred.

It has been shown in the literature that an unnecessary ICD shock may increase the mortality [24], which makes the detection of VT and VF and the identification of patients in the overlap zone crucial. With the proper identification of patients in the overlap zone, an ablation therapy could first be attempted due to considerable advances in catheter guidance methods [14, 30] for ablation. This does not suggest the ability to predict future arrhythmic episodes, but instead aid in optimizing treatment options based on present and past arrhythmic occurrences. Furthermore, this method could also be used to reduce the number of ICD discharges caused by inaccurate diagnosis of the Electrocardiogram (ECG), especially for patients suffering with an arrhythmia found in the overlap zone between VT and VF. The above forms a strong motivation in arriving at techniques that could analyze the ICD/surface ECG tracings and identify the overlap zone between VT and VF. The proposed work approaches the problem of identifying the overlap zone between VT and VF by quantifying the underlying organizational signal structures during an arrhythmia episode and determining the affinity toward a particular type of ventricular arrhythmia. Performing such affinity analysis in classifying the arrhythmias into VT or organized VF (OVF) or disorganized VF (DVF) will also enhance ICDs decision. For example, in cases where the arrhythmia is identified to be DVF (i.e., clearly not a misdiagnoses with fast paced VT), immediate shocking would be an appropriate choice that might save valuable time in avoiding pacing maneuvers before charging. Furthermore, this classification of previous arrhythmic episodes might assist the clinicians in deciding on future anti-arrhythmic drugs, multiple level shock threshold programming and ablation therapies. Recent studies [27] in atrial fibrillation (AF) show evidence that by identifying focal and spatially organized electrical activation patterns (rotors) and ablating them could modulate or terminate AF. In a similar vein, as a long-term treatment option, previous ICD shocks (i.e., previous arrhythmic episodes) can be analyzed by the clinician with a view to statistically identify the relative load of organized arrhythmia (especially OVF). Radio frequency ablation may be a therapeutic option in this subgroup.

There are many methods that exist when it comes to detecting and/or classifying ventricular arrhythmias into VT and VF. Time domain analyses such as dynamic sampling entropy [21], Empirical mode decomposition [1], ECG amplitude measure [19] and phase space reconstruction [32, 33] have been used to study and classify VF. Heart rate variability and RR interval are common features used in cardiology and arrhythmia classification, which is extracted by analyzing the inter-beat interval [5, 20, 28, 43]. VT and VF classification was also performed in the frequency domain by analyzing the dominant frequency (DF) [10], spatial derivative of DF [10], spectral coherence [34] and bandwidth [11] as well as DF harmonic analysis [7]. The majority of the above methods are accurate in their ability to separate VF and non-VF, and some [10, 31, 32, 34] are capable of classifying monomorphic VT, polymorphic VT from VF. However, due to the time-varying subtle signal structures that differentiate OVF and DVF, time-only or frequency-only techniques might not be sufficient to efficiently classify the OVF and DVF zone. Hence, it is evident that a more localized time–frequency domain technique must be used to be able to accurately distinguish the OVF overlap zone.

There are also works that have studied spatial organization, via 2D/3D electrical mapping of the heart, by constructing activation pattern maps [9, 17, 26], DF [10, 35], and phase maps [23, 35, 41, 42] to depict the temporal evolution of the spatial activation and organization. The proposed method differs from the above mentioned spatial mapping, because the current method focuses on the temporal organization using a single channel ECG to assist ICDs or clinicians in improving the treatment options for patients suffering from arrhythmias in the overlap zone of VT and VF. To the best knowledge of the authors, existing work pre-dominantly focuses on VT–VF classification, with little work [32–34] that focuses on the overlap zone that quantitatively detects monomorphic VT, polymorphic VT, and VF using surface ECGs. It is the sub-classification of VF into OVF and DVF that is challenging rather than VT and DVF, which is one of the main objectives of the proposed work.

2 Methodology

The methods are explained in five subsections. Details on the database used in this study are provided in Sect. 2.1, followed by brief descriptions on the continuous wavelet transform in Sect. 2.2 and singular value decomposition (SVD) in Sect. 2.3. Section 2.4 describes the feature extraction process to distinguish between VT, OVF, and DVF and Sect. 2.5 briefly explains the pattern classification approach.

2.1 Database

Due to the inherent difficulty (confidentiality and ethics approval) in obtaining ICD tracings of patients, this study develops and presents the methodology using surface ECG signals from the PhysioNet signal archives [15]. In particular, the Creighton University Ventricular Tachyarrhythmia Database as well as the MIT-BIH malignant ventricular arrhythmia database was used. A total of 63 4-s surface ECG segments with ventricular arrhythmias were

extracted from 24 patients. These signals were then filtered between 0.3 and 30 Hz [40]. The signals were normalized to reduce the variance between the average signal levels. These signals were pre-classified as VT, OVF (predominantly early VF), and DVF (predominantly late VF) by trained electrophysiologists at the Toronto General Hospital, Toronto, Canada which served as the gold standard. Of the 63 signals, 21 were categorized into VT, 20 into OVF, and 22 as DVF.

2.2 Continuous wavelet transform (CWT)

To quantify the organizational signal structures of a signal, it is essential to study the joint time–frequency/time-scale properties of the signal. Although there are several time–frequency/time-scale analysis methods available, the use of the wavelet transform is appropriate due to the flexibility in the choice of mother wavelets to capture specific time-scale structures in the ECG, which is crucial for time varying or non-stationary signal analysis. The most significant aspect that makes the wavelet transform better suited is its ability to naturally vary the window size. This is important because it allows the mother wavelet to use an appropriate window size to analyze a particular frequency. Since the window is changing for a given frequency, it inherently has its advantages in localizing the occurrence of a particular frequency/scale over time [22]. For these reasons the proposed method uses wavelet analysis.

In CWT, a signal $x(t)$ can be expressed as a combination of scaled (dilated) and translated version of a mother wavelet ψ. The continuous wavelet transform is given by Eq. 1 [2, 22].

$$C_{x(t)}(a,b) = \frac{1}{\sqrt{a}} \int_{-\infty}^{\infty} x(t)\psi^*\left(\frac{t-b}{a}\right)\mathrm{d}t \tag{1}$$

The parameter a represents the scaling (inversely related to frequency) parameter and b represents the translation parameter of the wavelet. The wavelet that was used in this study was the complex Morlet wavelet. The reason for using an analytic wavelet instead of a real wavelet is that they are better suited for studying the frequency evolution of the signal $x(t)$ through time [22]. The discrete time continuous wavelet transform (DT-CWT) was used for the analysis of the ECG, which is given in Eq. 2 [4].

$$C_{x(n)}(a',b') = \frac{1}{\sqrt{a'}} \sum_{n=0}^{N-1} x(n)\psi\left(\frac{n-b'}{a'}\right) \tag{2}$$

The variables a' and b' represents the discretized scale and time parameter for the mother wavelet, n represents the time index and N represents the length of the signal $x(n)$. To eliminate the influence of energy variations between signals, matrix $C_{x(n)}(a', b')$ was normalized. The normalization was done by representing each node in the coefficient as a percentage of the total energy captured and is given by Eq. 3.

$$\hat{C}_{x(n)}(a',b') = \frac{100 \times (|C_{x(n)}(a',b')| \times |C_{x(n)}(a',b')|)}{\sum_{a'}\sum_{b'} (|C_{x(n)}(a',b')| \times |C_{x(n)}(a',b')|)} \tag{3}$$

Three real arrhythmia samples from the MIT database were analyzed using the wavelet transform to give us a time-scale representation of the groups. Figure 1a–c shows three sample surface ECGs pre-classified by the electrophysiologist as a VT, OVF, and DVF ECG episode. From Fig. 1a (top and bottom panels), it can be observed that VT has a strong organized structure because the signal energy is confined to a narrow bandwidth but spreads uniformly over time. The DVF example in Fig. 1c (top and bottom panels) does not have an observable organizational structure and the energy is distributed over the time-scale plane (disorganized). This is also reflected in the scalogram (bottom panel of Fig. 1c). Visually inspecting the OVF ECG, and the scalogram found in the bottom panel of Fig. 1b, it can be observed that there is a higher degree of organization than the DVF example found in Fig. 1c, because most of the scalogram energy in the OVF example is confined to a smaller range of scales. However, it is not as organized as the VT example in Fig. 1a since the energy in the confined scales is not consistent through time in the scalogram.

Since VF is non-stationary in nature, wavelet transform is suitable for the task due to its time-scale properties and has been successfully applied in existing literature for VF analysis [12, 18, 37, 44, 49] and it is also computationally less expensive. Initial results of the ventricular arrhythmia classification into VT, OVF, and DVF were presented in [6], where image processing was applied to the wavelet scalogram (as seen in Fig. 1) to capture dominant energy peaks. The proposed study provides an analysis of the wavelet scalogram of the ECG using singular value decomposition (SVD). Features extracted from the SVD are used to classify VT and further sub-classify non-VT into OVF and DVF. Using SVD on the wavelet time-scale/time–frequency plane for extracting features is a known approach and has been applied by existing works [16, 25, 45].

2.3 Singular value decomposition

The differences in the arrhythmia signal structures (both in the time domain and in the time-scale domain) for VT, OVF, and DVF groups can be observed from Fig. 1. SVD can be applied to the time-scale plane such that discriminative features can be extracted to capture the group characteristics found in the scalogram. SVD decomposes

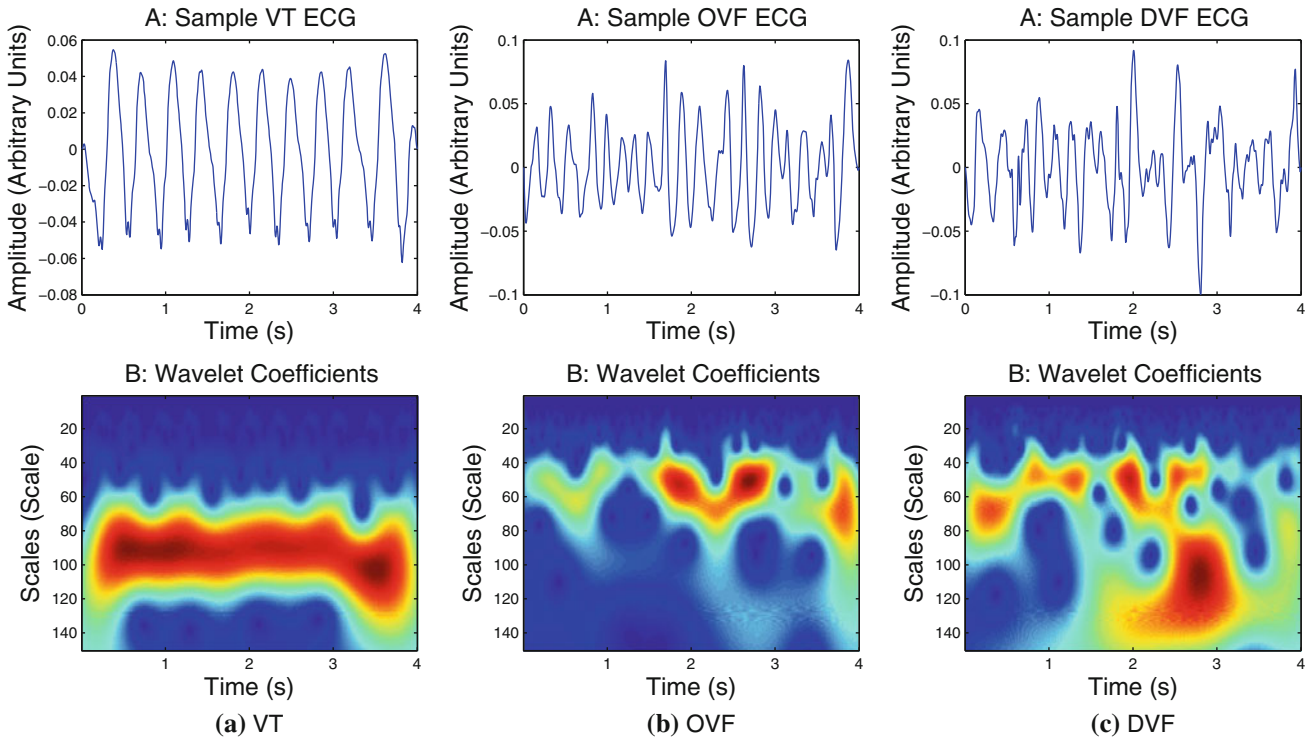

Fig. 1 Examples of ECGs depicting VT (**a**), OVF (**b**) and DVF (**c**)

the information spread over the time-scale plane by treating the scalogram matrix as a sum of separable components [45]. Briefly, the concept behind SVD is to decompose the matrix $\hat{C}_{x(n)}(a',b')$ (shown in Eq. 3) into a canonical form. The canonical form decomposes the matrix into the format given in Eq. 4 [3]. The indices c in the matrix $\hat{C}_{x(n)}(a',b')$ give the percentage of energy captured by the Morlet wavelet at a particular time and scale.

$$\hat{C}_{x(n)}(a',b') = USV^{\mathrm{H}} \tag{4}$$

The matrices U and V are unitary matrices and H denotes the complex conjugate transpose of the matrix. The singular values are represented by S. Therefore, the scalogram matrix $\hat{C}_{x(n)}(a',b')$ is factorized by creating two unitary matrices, U and V, and a singular value diagonal matrix S [8]. The matrices U and V^{H} represent components that describe the energy distribution pattern found in the scalogram $\hat{C}_{x(n)}(a',b')$. The singular values in the matrix S represent the amount of energy captured by the components U and V^{H} from the scalogram $\hat{C}_{x(n)}(a',b')$. The matrices U and V^{H} have a unique representation when SVD is applied to the scalogram. If the scalogram is oriented such that the rows contain the frequency aspects and the columns contain the time aspects of the scalogram, then the U matrix (of size A') contains the components that capture the spectral information (in terms of scales) and the V^{H} matrix (of size B') has the components that capture the temporal information. Equations 5 and 6 show how U and V capture the spectral and temporal information.

$$\hat{C}_{x(n)}(a',b') \times \hat{C}_{x(n)}(a',b')^{\mathrm{T}} = US'U^{\mathrm{T}} \tag{5}$$

$$\hat{C}_{x(n)}(a',b')^{\mathrm{T}} \times \hat{C}_{x(n)}(a',b') = VS''V^{\mathrm{T}} \tag{6}$$

Both the U and V matrices perform an Eigen Decomposition on the matrices $\hat{C}_{x(n)}(a',b') \times \hat{C}_{x(n)}(a',b')^{\mathrm{T}}$ and $\hat{C}_{x(n)}(a',b')^{\mathrm{T}} \times \hat{C}_{x(n)}(a',b')$, respectively [39]. U and V obtain the Eigen vectors of their respective matrices to calculate the components. The Eigen values S' and S'' contain the same non-zero diagonal entries of matrix S, but may be placed in a different order. The matrices $\hat{C}_{x(n)}(a',b') \times \hat{C}_{x(n)}(a',b')^{\mathrm{T}}$ and $\hat{C}_{x(n)}(a',b')^{T} \times \hat{C}_{x(n)}(a',b')$ identify the dominant energy structures from both the scale and time, respectively. Therefore, performing the Eigen decomposition of these matrices allows for the identification of the prominent signal structures, which is represented in the Eigen vectors that are obtained. The eigen values would then indicate which component is more dominant for the given scalogram.

For the scalogram given in Eq. 7, each U and V^{H} component capture specific energy variation from the matrix $\hat{C}_{x(n)}(a',b')$. Therefore, for a particular component i, the combination of the U and V^{H} with the corresponding singular value can create the scalogram that captures a

particular set of energy variations from $\hat{C}_{x(n)}(a', b')$. Equation 8 shows that the ith column of matrix U multiplied by the ith row of matrix V^{H} multiplied by the corresponding singular value creates the filtered version of the scalogram $\hat{C}_{x(n)}(a', b')$.

$$\begin{array}{|c|c|c|c|} \hline c_{1,1} & c_{1,2} & \cdots & c_{1,b} \\ \hline c_{2,1} & c_{2,2} & & \\ \hline \vdots & & \ddots & \\ \hline c_{a,1} & & & c_{a,b} \\ \hline \end{array} = \hat{C}_{x(n)}(a', b') \tag{7}$$

$$\hat{C}_{x(n),i}(a', b') = U_{a',i} \times S_{i,i} \times V^{\mathrm{H}}_{i,b'} \tag{8}$$

There are many existing works where SVD has been used to obtain information on a given wavelet scalogram. SVD was used to determine the ridges from the CWT [29]. The ridges of the wavelet transform play a key role in determining the phase structure, and this was captured using the dominant SVD components to find the local maxima in the scalogram. In [16], SVD of information spread over the time–frequency plane was used to classify EEG seizure in newborn infants. In [25], a wavelet-SVD analysis on normal sinus ECGs with support vector machine-based classifier was used to predict the occurrence of a type of cardiac arrhythmias. The proposed method, on the other hand, analyzes the surface ECG during an arrhythmia episode to determine its organizational structure.

To demonstrate the power of SVD decomposition on the scalogram, two synthetic signals were created, the first signal simulates a Monomorphic VT signal (a sinusoid), and the second signal simulates the DVF signal. The third signal is from a patient suffering from a DVF episode. Part A of Fig. 2a, b and c shows the scalogram of the simulated VT and DVF and real world DVF signal, respectively, along with the first five components from both the U and V^{H} matrix and the line plot of the first dominant component for each matrix (shown above the rows of the V^{H} matrix and to the left of the columns of the U matrix) in part B and C, respectively. The original time-domain signal is also given in part D of the figures.

The set of first components which consists of the first column of the U matrix (Part B of Fig. 2a–c) and the first row of the V^{H} matrix (part C of Fig. 2a–c), can be observed to capture specific information with regards to the scalogram. In particular, it captures the most dominant localized energy variation within the scalogram. For example, in Fig. 2a, the energy distribution in the first component of the U matrix (line plot in part B of Fig. 2a) is centered between the scales of 40 and 60, where as the component in the V^{H} matrix (line plot in part C of Fig. 2a) has its energy distributed throughout the time window. Figure 2b, however, shows that the energy distribution in the first component of the U matrix (line plot in part B of Fig. 2b) is spread across multiple scales and the first component of the V^{H} matrix (line plot in part C of Fig. 2b) is not as distributed (comparatively) through time. SVD has accurately captured the dominant component found in the synthesized signals. The singular values give an indication of the amount of energy retained by each component [46]. SVD then reorganizes the components such that they are sorted in descending order of the singular values. The similarities of the SVD characteristics (dominant U and V^{H} components) between the synthetic DVF (Fig. 2b) and the DVF obtained from a patient (Fig. 2c) can be easily observed. Therefore, discriminant features for the arrhythmias (VT, OVF and DVF) could be obtained by analyzing the dominant component captured by the U and V^{H} matrix as well as the dominant component's singular value.

2.4 Feature extraction

The extraction of the features allows us create a two-level binary classification system to categorize the arrhythmia groups. The first classification level provides features that can separate VT from non-VT ECGs. The second level can focus on further sub-classifying the non-VT ECGs into OVF and DVF.

2.4.1 Features 1 and 2: first component singular value and first V component variance analysis

An observable difference between the VT and non-VT groups from the SVD of scalogram is that the energy distribution in the first component of the V^{H} matrix of a VT signal is expected to be equally distributed for most of the time (which could be observed in part C of the simulated VT signal in Fig. 2a). Since VT can also be modeled using fewer components, it makes the initial singular value for these components to be much larger than the subsequent components. In the case of a non-VT signal, the energy distribution in the first component of the V^{H} matrix will be non-uniform and relatively larger number of components will be required to represent the scalogram, which in turn makes the singular values more spread over subsequent components unlike VT. The features that can be used to classify VT from non-VT ECGs would be the percentage of energy captured by the first component (refer to $F1$ from Eq. 9) and the variance of the first component (i.e., first row) of the V^{H} matrix ($F2$ from Eq. 10).

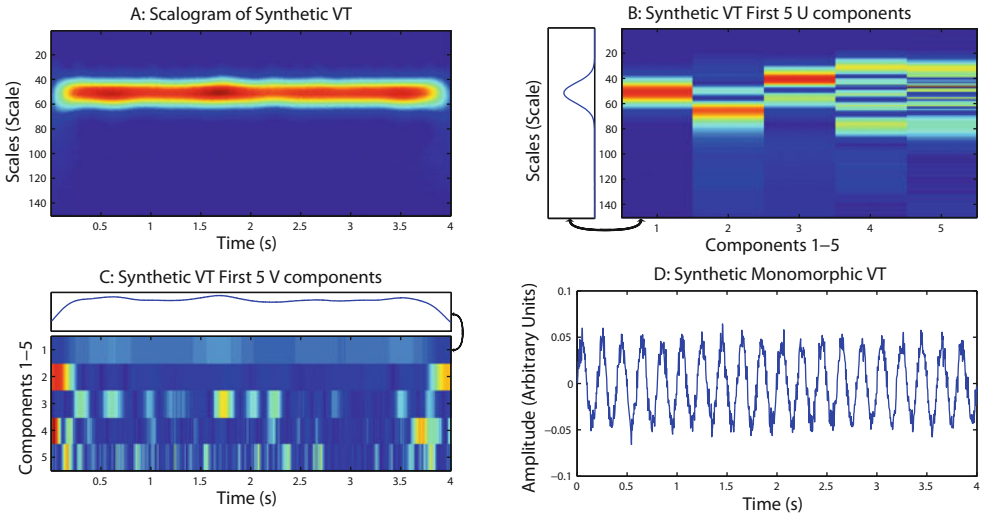

(a) Simulated VT

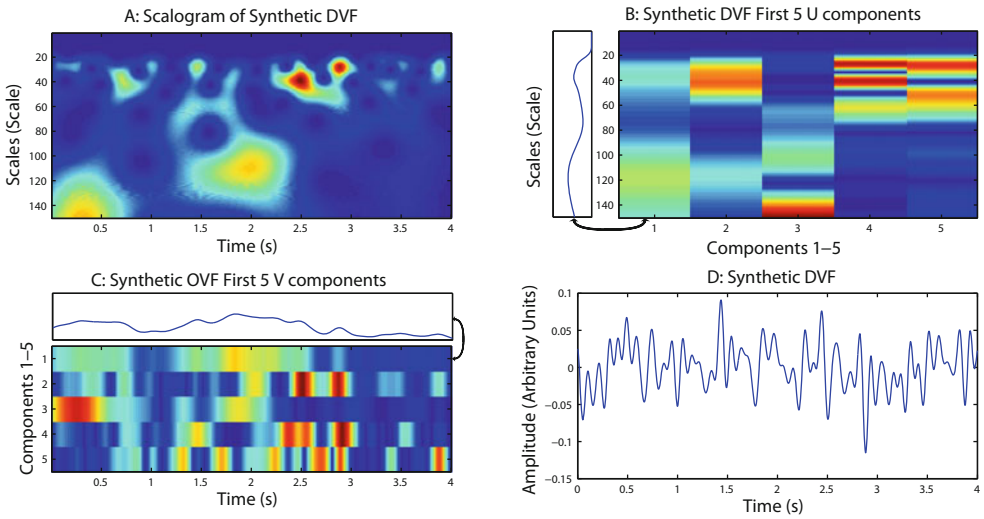

(b) Simulated DVT

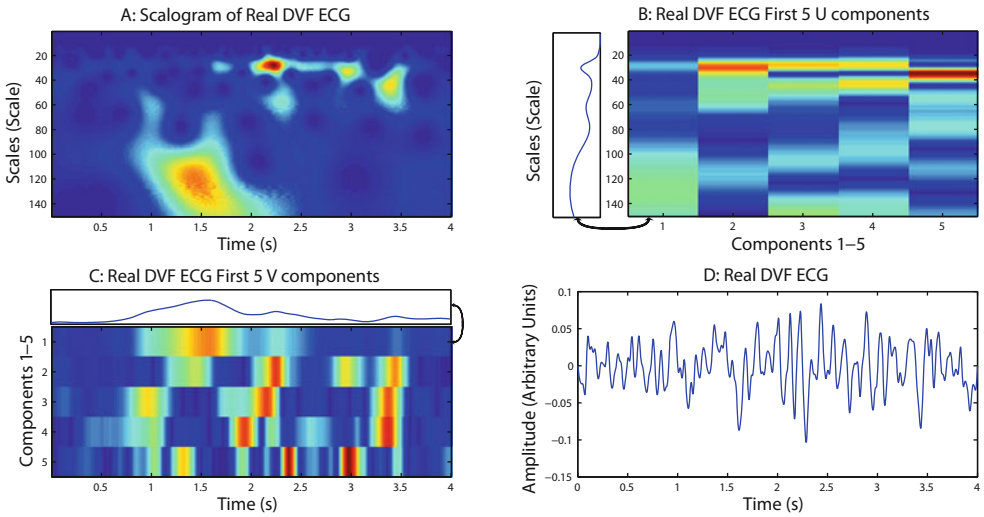

(c) Real DVT Sample

Fig. 2 SVD analysis of simulated VT (**a**) and DVF (**b**) and a real DVF (**c**) ECG

$$F1 = \hat{S}_i = \frac{S_i}{\sum_{j=1}^{r} S(j)} \tag{9}$$

$$F2 = \sigma^2_{V,i} = \frac{1}{B' - 1} \sum_{k=1}^{B'} (|V^{\mathrm{H}}(k,i)| - \bar{V}^{\mathrm{H}}) \tag{10}$$

In Eq. 9, $\hat{S}$ represents the singular value for component i expressed as a percentage and r represents the rank of $\hat{C}_{x(n)}(a', b')$ $(r \leq \min\{A', B'\})$. A' and B' represent the maximum values for parameters a' and b' respectively. The percentage of the singular value is used instead of the actual value because the value produced by taking the SVD of a matrix gives specific information about the scalogram and cannot be directly used for comparison. The percentage is indicative of how much energy is captured by the particular U and V^{H} component. In Eq. 10, σ^2 represents the variance of vector V^{H}, $\bar{V}^{\mathrm{H}}$ is the mean of the vector $|V^H|$ for component i.

2.4.2 *Feature 3: first U component variance analysis*

As explained in the previous section, non-VT ECGs can be segregated using features $F1$ and $F2$ (percentage of energy captured by dominant component and first component in the V^{H} matrix). The most distinguishing feature between the OVF and DVF was observed in their composition of organized signal structures which is reflected in the energy distribution of the dominant component of U matrix. This was also observed directly from the scalogram of the OVF and DVF ECG (Fig. 1). As DVF is dis-organized with multiple frequency components, it has a highly varying energy distribution over frequency relative to OVF, which had few narrower peaks. This is captured in the dominant (first) component of the U matrix. Hence, the variance of the dominant component of U will therefore be a suitable feature in classifying the organization range of VF. The feature $F3$ using Eq. 11 was extracted for this purpose (similar to the extraction of $F2$).

$$F3 = \sigma^2_{U,i} = \frac{1}{A' - 1} \sum_{j=1}^{A'} (|U(i,j)| - \bar{U}) \tag{11}$$

Features relating to energy distribution over the signal's Fourier spectrum, similar to the above feature obtained from the U matrix, could also be extracted and used for OVF and DVF classification. The first significant difference of this feature is that only the dominant scale components are analyzed for their spread, as opposed to capturing the total energy distribution from the signals Fourier spectrum. In addition to the time-scale properties, the advantages of using the wavelet transform are that it provides the flexibility to choose different mother wavelets which could be used to emphasize or de-emphasize certain signal characteristics and the information extracted from the U matrix is actually in terms of scales (inversely related to frequency) and can be easily associated to morphological signal structures of interest.

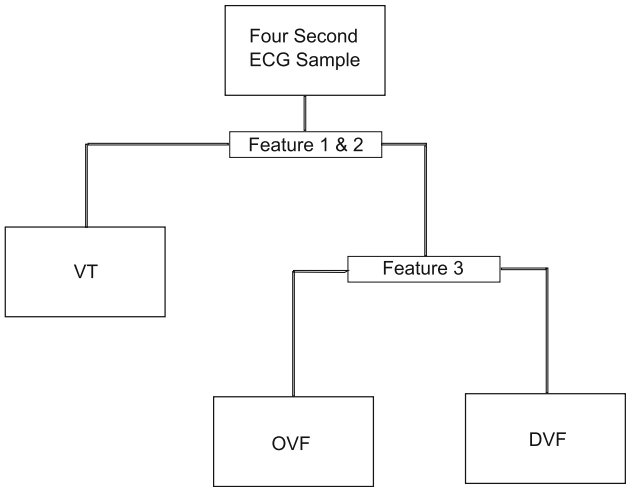

Fig. 3 Two-level binary classification

2.5 Pattern classification

The proposed 2-level binary classification is illustrated in Fig. 3. The extracted features, explained in Sect. 2.4, were fed to a linear discriminant analysis (LDA) based classifier [38]. To effectively test the robustness of the classifier, cross validation was performed using the leave-one-out (LOO) method [13]. In the LOO method, the classifier is trained with all samples except one and the single sample is used for testing. This is repeated by leaving out each of the samples in the database, training the classifier with the remaining samples, and computing the classification. The classification accuracy is then computed as the average of classification accuracies obtained by leaving out each of the samples. Two sets of classification accuracies were obtained because a binary classifier was used.

3 Results

The first level classification was made to distinguish between VT and non-VT groups. The second level classification was performed to distinguish between DVF and OVF. Figure 4 represents the scatter plot, using $F2$ (the first V^{H} component variance distribution) and $F1$ (the first component singular value percentage), that distinguishes VT from non-VT groups. The linear boundary separating VT and the rest is obtained from the classification and shown in Fig. 4. VT scalograms typically have uniform energy distribution across time, thus making the $F2$ (X axis

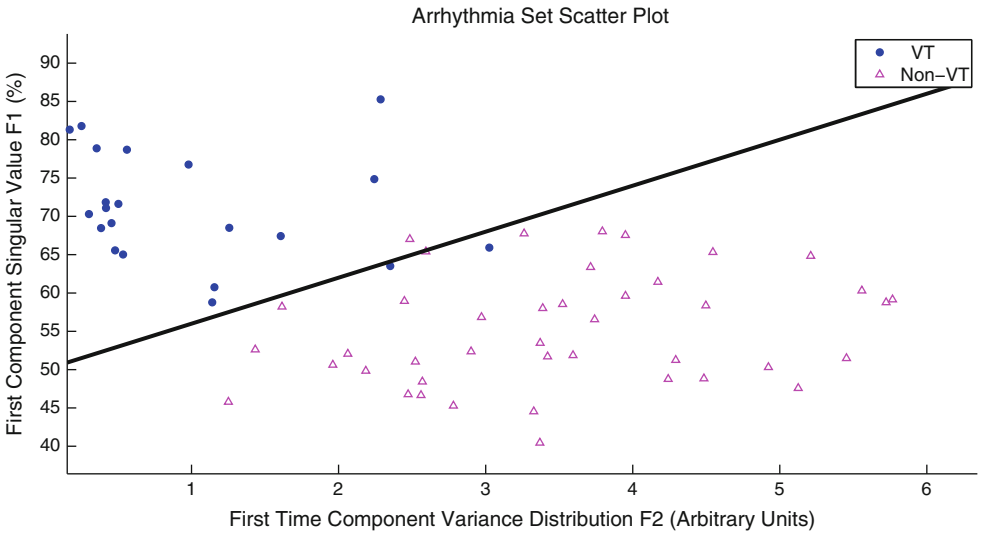

Fig. 4 Arrhythmia scatter plot for VT and non-VT

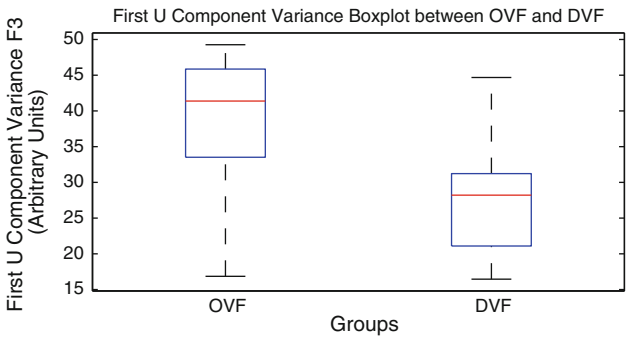

Fig. 5 *Box plot* of the variance of the first U component between OVF and DVF

from Fig. 4) lower when compared to the non-VT signals. Furthermore, since VT requires fewer number of components to model, the $F1$ (Y axis from Fig. 4) shows that all VT samples have a relatively higher first singular value when compared to non-VT group. Hence VT signals occupy the top left corner of the scatter plot.

The feature used to distinguish between OVF and DVF was the energy distribution of the first U component ($F3$). Since this classification uses one feature, a box plot shows the distribution of the feature for the two groups. Figure 5 demonstrates the classification of OVF and DVF using $F3$ (variance of the first dominant scale component). It is observed that OVF tends to have a higher variance than DVF due to OVF dominant component typically having fewer and narrower spectral peaks.

LOO cross validation was performed in estimating the classification accuracy. For the first level of the binary classification, an accuracy of 93.7 % was obtained. The confusion matrix for the classification is presented in Table 1. Out of the 21 VT signals, 19 were correctly classified with accuracy of 90.5 % and out of the 42 non-VT signals, 40 were correctly classified with an accuracy of 95.2 %.

Table 1 Level 1 binary classification

Method	Groups	VT	Non-VT	Total
Cross-validated	VT	**19**	2	21
	Non-VT	2	**40**	42
%	VT	**90.5**	9.5	100
	Non-VT	4.8	**95.2**	100

Cross-validated, linear discriminant analysis with leave-one-out method; %, percentage of classification

The number (and %) in bold values indicate the number (and %) of cases correctly classified in the respective groups

The second level of the classification achieved a classification accuracy of 80.0 %. The confusion matrix for the classification is presented in Table 2. Out of the 18 OVF signals, 14 were correctly classified with accuracy of 77.8 % and out of the 22 DVF signals, 18 were correctly classified with an accuracy of 81.8 %. Considering the difficulties in discriminating between subgroups of VF into OVF and DVF, the obtained results are encouraging.

The results from the proposed feature in the classification of OVF and DVF were compared with that of spectral features (DF power and bandwidth with a classification accuracy of 63.15 %), and found that it is much lower than the proposed feature. The proposed features were also tested in a single classification system, as opposed to a binary classifier, and an overall classification accuracy of 79.4 % was obtained for a direct three group classification into VT, OVF and DVF.

In addition, to illustrate the significance of the proposed method in its application of identifying the overlap zone, ECGs of two patients that contained markers for the onset of VF from the MIT database were tested to study the occurrences of OVF and DVF. The first 60 s and the last 60 s of the VF episodes were tested by analyzing a 4-s sliding window (113 window segments each minute with a

Table 2 Level 2 binary classification

Method	Groups	OVF	DVF	Total
Cross-validated	OVF	**14**	4	18
	DVF	4	**18**	22
%	OVF	**77.8**	22.2	100
	DVF	18.2	**81.8**	100

Cross-validated, linear discriminant analysis with leave-one-out method; %, percentage of classification

The number (and %) in bold values indicate the number (and %) of cases correctly classified in the respective groups

Table 3 OVF and DVF occurrences in two patients

	First 60 s	Last 60 s
Patient 1		
OVF occurrences	**113**	18
DVF occurrences	0	**95**
Total segments	113	113
Patient 2		
OVF occurrences	**105**	40
DVF occurrences	8	**73**
Total segments	113	113

The number (and %) in bold values indicate the number (and %) of cases correctly classified in the respective groups

3.5 s overlap between adjacent windows) for the number of OVF/DVF occurrences. On average, there were a higher number of OVF occurrences in the first 60 s of the onset of VF compared to the last 60 s. The results of this analysis are presented in Table 3. The global organization (or average organization) can be seen as a transition from OVF to DVF in both instances. This shows that the proposed method can be used to study the overlap zone more accurately, to aid in the prognosis of the patient.

3.1 Comparative analysis

A comparative analysis with existing works on arrhythmia classification was performed to benchmark the performance of the proposed method. The algorithms proposed by Ropella et al. [34] and by Roberts et al. [31, 32] were tested due to their ability to classify MVT, PVT and VF. The algorithm developed by Namarvar et al. [25] was also implemented due to its similarity to the proposed method, although their motivation was on arrhythmia prediction using normal sinus ECGs. These methods were compared for a number of characteristics and these are highlighted in Table 4. For the classification accuracy comparison, all the methods were tested with an uniform 4-s window.

The spectral coherence and phase space reconstruction methods were tested on a smaller subset of the database, because these methods require dual lead information (which was unavailable for some patient ECGs in the public databases used in this study). For the comparison to be fair, the proposed method was also tested on the same smaller subset of the database. The method proposed by Namarvar et al. [25] was tested on the full database, as single lead information was sufficient for implementing

Table 4 Comparative analysis

Method	Electrogram/ECG in original work	Number of leads used	Analysis type in original work	Analysis domain	Analysis time segment (s) in original work	Target classification in original work	Feature dimensionality	Classification of VT, OVF, DVF in this study	
								VT/non-VT (%)	OVF/DVF (%)
Proposed method	Surface	1	Arrhythmia classification	Time-scale	4	VT, OVF and DVF	3	97.1[a]	85.7[a]
Phase space reconstruction [31, 32]	Surface	2	Arrhythmia classification	Time	2.5	MVT, PVT and VF	101	85.7[a]	57.1[a]
Spectral coherence [34]	Intra-cardiac	2	Arrhythmia classification	Frequency	4.24	MVT, PVT and VF	1	60[a]	53.8[a]
Wavelet-SVD-SVM [25]	Surface	1	Arrhythmia prediction	Time-scale	1.024	VT and VF prediction from sinus rhythm	U matrix ($A' \times A'$ features)	83.87[b]	73.80[b]

[a] Binary classification on smaller database with dual leads (35 samples with 13 VT, 7 OVF and 15 DVF)

[b] Binary classification using the full database (since it used only a single lead, which is same as the proposed method), SVM and the scale unitary matrix (U) with $A' \times A'$ number of features. The results of 83.87 % for VT/non-VT and 73.80 % for OVF/DVF achieved by this method should be compared to 93.7 and 80 % of the proposed method using the full database

this method. The wavelet used in the comparative analysis for the method proposed by Namaravar et al. [25] was the complex Morlet and a linear kernel was used for the SVM classifier.

The results for the different methods are highlighted in the last column of Table 4. The results given are the binary LOO classification accuracies. From the results, it can be observed that the proposed method performs well in comparison to the spectral coherence and the phase space reconstruction methods on the smaller subset of the original database (97.1 and 85.7 % compared to 60 and 53.8 % for spectral coherence and 85.7 and 57.1 % for phase space reconstruction). It should be noted that the spectral coherence method and phase space reconstruction performed especially poor in the classification of OVF and DVF. The feature identified by Narmarvar et al. [25] (unitary matrix representing the scale energy of the wavelet coefficients) provided a VT/non-VT classification of 83.87 % and an OVF/DVF classification accuracy of 73.80 % on the full database. However, the classification of VT samples was only 47.62 %. Similarly, the OVF classification was found to be 61.90 %. These results are lower when compared to the VT and OVF classification results of the proposed method from Tables 1 and 2 (90.5 and 77.8 %, respectively).

4 Discussion

Ventricular arrhythmias seriously affect the quality of life and could be lethal and lead to sudden cardiac death. Arriving at techniques that could perform automated classification of ventricular arrhythmias in a short period of time has significant implications in the choice of therapies and survival rates of patients. Our results suggest that the proposed method using features derived from the time-scale plane performs well in classifying ventricular arrhythmias, and in particular the highlight of the work being the sub-classification of VF into OVF and DVF to identify the overlap zone. This could be of immense assistance to ICDs and clinicians in optimizing treatment options for the affected population with an arrhythmia in the overlap zone.

Recent studies [10, 23, 35, 41, 42] have indicated the presence of spatio-temporal organization during VF and have associated them to the sources that maintain VF. It has also been shown that the ablation of centers of organization (rotors) during AF could terminate AF [27]. The manifestation of these organized activities on the surface ECG during VF could be related to the presence of signal components that have time–frequency/time-scale patterns. Quantifying and studying these time-scale/time–frequency components could provide a better metric on the transition from organized VT to disorganized VF rather than rate-dependent approaches. Our methodology achieves this using wavelet-SVD analysis on surface ECGs where we focus on the deriving features from dominant signal components in the time-scale plane (i.e., both from time and scale dimensions) and arrive at an organization index. It has also been shown in literature [36] that the transition from VT to VF has a relation to the spatial organization and short-lived rotors [36, 42], and therefore validates the need for an overlap zone to better capture this transition. Our results also confirm this, as our technique identified more OVF segments during early VF and more DVF segments during the later stages of VF.

In comparison with few of the related techniques [25, 31, 32, 34], the proposed method in overall performs well with the given database (either a subset or full) and for the proposed target classification. It could be observed that the majority of the existing methods did perform comparatively well for VT/non-VT classification; however, their performance in classifying OVF–DVF is below the proposed method. Based on our features and analysis presented in this work, it is evident that we operate on a filtered (i.e., dominant sub-plane) time-scale plane that correspond to the dominant U (spectral) and V (temporal) vectors. In other words, we operate on a set of dominant signal components that have specific time and frequency localization. Relating this to spectral techniques [7, 10, 11, 34], they are limited in operating only on the global spectrum of the signals, which does not allow them to extract spectral information for selective time-scale components that may be of interest. This could explain the lower performances of these techniques for the proposed classification. In addition, the spectral coherence method [34] uses dual channel information while the proposed method performs well using a single-channel ECG. The phase space reconstruction [31, 32] method also had difficulties in classifying OVF and DVF while it performs relatively well for VT-non-VT classification. Since in this method the correlation between the ECG leads (requires dual lead) is the key to the discrimination, the subtle morphological differences between the OVF and DVF may not be captured effectively.

The method proposed by Narmarvar et al. [25] performs with comparable results to the proposed method. However, closely analyzing the results indicates a poor classification of VT and OVF. As discussed earlier our proposed method derives features from both temporal and spectral dimensions whereas the work proposed by Narmarvar et al. [25] only operates on the *U* matrix which corresponds to spectral information. From the results presented in this study, for VT and non-VT classification an important feature is the time-support of the dominant time-scale component and the information of which lies in

the V matrix. Excluding the information from the V matrix could explain the lower performance of their work in classifying VT and non-VT group. The other important differences are the dimensionality of the feature space and that they used normal sinus ECGs in predicting arrhythmias. With respect to dimensionality, using the U unitary matrix in its entirety produces a large feature space [depending on the scale range ($A' \times A'$)], whereas the proposed algorithm in this study has derived features only from the dominant time-scale components and selected three features from it.

It should be noted that the poor performance of the above discussed methods could also be attributed to the small database size (spectral coherence and phase space reconstruction methods) due to the requirement of dual lead information and that their target classification groups were different to that of the proposed method. However, since they were all tested in a similar setting (either with a subset or full database), it is fair to say that although all the methods perform comparatively well in VT–non-VT classifications, the proposed method using a single lead ECG demonstrates higher potential in classifying the OVF–DVF group accurately. This could result in a tool that the clinician can use to discriminate the organization levels between the three types of arrhythmias. Although the method used was demonstrated on surface ECG with arrhythmic episodes, it could easily be extended to analyze tracings from ICDs, because ICD tracings would still preserve the organization aspects of the three groups.

A limitation to the proposed method is that the tool presented in this article cannot be used as a risk-stratifier to determine whether a patient should get an ICD or not. The techniques presented here cannot determine the probability of future VF episodes, but can aid in classifying past and present arrhythmic events and provide the clinician with a better understanding of the type of arrhythmia that the patient may be faced with.

5 Conclusion

The proposed study presented a wavelet-SVD based method to classify ventricular arrhythmias and in particular the overlap zone between VT and VF. This could aid clinicians in diagnosing those patients who suffer from arrhythmias in the overlap zone and suitably provide them with optimal therapeutic solutions. The proposed approach can also aid ICDs in choosing appropriate therapy based on an organizational index rather than the current rate-dependent detectors of arrhythmias. A comparative analysis with the related existing methods illustrates that the proposed method has higher potential in sub-classifying VF into OVF and DVF. Future work involves identifying the discriminatory time-scale patterns that could be associated with mechanism that initiates and maintains VF.

Acknowledgments The authors would like to thank the Hull family cardiac fibrillation management laboratory, Toronto General Hospital, and in particular Dr K. Nanthakumar for his expert opinion on this work. The authors also thankfully acknowledge Natural Sciences & Engineering Research Council of Canada (Grant to Dr. K. Umapathy) for supporting this work.

References

1. Abdullah Arafat M, Sieed J, Kamrul Hasan M (2009) Detection of ventricular fibrillation using empirical mode decomposition and bayes decision theory. Comput Biol Med 39(11):1051–1057
2. Addison P (2005) Wavelet transforms and the ecg: a review. Physiol Meas 26:R155
3. Akritas A, Malaschonok G, Vigklas P (2006) The svd-fundamental theorem of linear algebra. Nonlinear Anal 11(2):123–136
4. Angrisani L, Daponte P, D'Apuzzo M, Testa A (1998) Ameasurement method based on the wavelet transform for power quality analysis. IEEE Trans Power Del 13(4):990–998
5. Asl B, Setarehdan S, Mohebbi M (2008) Support vector machine-based arrhythmia classification using reduced features of heart rate variability signal. Artif Intell Med 44(1):51–64
6. Balasundaram K, Masse S, Nair K, Farid T, Nanthakumar K, Umapathy K (2011) Wavelet-based features for characterizing ventricular arrhythmias in optimizing treatment options. In: Engineering in Medicine and Biology Society, 2011. IEMBS'11. 33rd Annual international conference of the IEEE, vol 1. IEEE, New York, pp 969–972
7. Barquero-Pe′rez O′, Rojo-Alvarez J, Caamañ o A, Goya-Esteban R, Everss E, Alonso-Atienza F, Sa′nchez-Munoz J, Garc′ıa-Alberola A (2010) Fundamental frequency and regularity of cardiac electrograms with fourier organization analysis. Biomed Eng IEEE Trans 57(9):2168–2177
8. Casey M (1998) Auditory group theory with applications to statistical basis methods for structured audio. Ph.D. thesis, Massachusetts Institute of Technology
9. Cheng K, Dosdall D, Li L, Rogers J, Ideker R, Huang J (2012) Evolution of activation patterns during long-duration ventricular fibrillation in pigs. Am J Physiol Heart Circ Physiol 302(4):H992–H1002
10. Ciaccio E, Coromilas J, Wit A, Garan H (2011) Onset dynamics of ventricular tachyarrhythmias as measured by dominant frequency. Heart Rhythm 8(4):615–623
11. Clayton R, Murray A, Campbell R (1994) Changes in the surface electrocardiogram during the onset of spontaneous ventricular fibrillation in man. Eur Heart J 15(2):184
12. Foomany FH, Umapathy K, Krishnan S, Masse S, Farid T, Nair K, Dorian P, Nanthakumar K (2010) Wavelet-based markers of ventricular fibrillation in optimizing human cardiac resuscitation. In: Conference proceedings: IEEE Engineering in Medicine and Biology Society, pp 2001–2004
13. Fukunaga K (1990) Introduction to statistical pattern recognition. Academic Press, New York
14. Fukuoka Y, Oostendorp T, Armoundas A (2009) Method for guiding the ablation catheter to the ablation site: a simulation and experimental study. Med Biol Eng Comput 47(3):267–278
15. Goldberger AL, Amaral LAN, Glass L, Hausdorff JM, Ivanov PC, Mark RG, Mietus JE, Moody GB, Peng CK, Stanley HE (2000) PhysioBank, PhysioToolkit, and PhysioNet: components of a new research resource for complex physiologic signals.

Circulation 101(23):e215–e220. http://circ.ahajournals.org/cgi/content/full/101/23/e215
16. Hassanpour H, Mesbah M, Boashash B (2004) Time-frequency feature extraction of newborn eeg seizure using svd-based techniques. EURASIP J Appl Signal Process 2004:2544–2554
17. Huang J, Rogers J, Killingsworth C, Singh K, Smith W, Ideker R (2004) Evolution of activation patterns during long-duration ventricular fibrillation in dogs. Am J Physiol Heart Circul Physiol 286(3):H1193
18. Khadra L, Al-Fahoum A, Al-Nashash H (1997) Detection of life-threatening cardiac arrhythmias using the wavelet transformation. Med Biol Eng Comput 35(6):626–632
19. Krasteva V, Jekova I (2005) Assessment of ecg frequency and morphology parameters for automatic classification of life-threatening cardiac arrhythmias. Physiol Meas 26:707
20. Lerma C, Wessel N, Schirdewan A, Kurths J, Glass L (2008) Ventricular arrhythmias and changes in heart rate preceding ventricular tachycardia in patients with an implantable cardioverter defibrillator. Med Biol Eng Comput 46(7):715–727
21. Li H, Han W, Hu C, Meng M (2009) Detecting ventricular fibrillation by fast algorithm of dynamic sample entropy. In: Robotics and Biomimetics (ROBIO), 2009 IEEE International Conference. IEEE, New York, pp 1105–1110
22. Mallat S (1999) A wavelet tour of signal processing. Academic Press, New York
23. Masse' S, Downar E, Chauhan V, Sevaptsidis E, Nanthakumar K (2007) Ventricular fibrillation in myopathic human hearts: mechanistic insights from in vivo global endocardial and epicardial mapping. Am J Physiol Heart Circ Physiol 292(6):H2589
24. Mishkin J, Saxonhouse S, Woo G, Burkart T, Miles W, Conti J, Schofield R, Sears S, Aranda J Jr (2009) Appropriate evaluation and treatment of heart failure patients after implantable cardioverter-defibrillator discharge: time to go beyond the initial shock. J Am Coll Cardiol 54(22):1993–2000
25. Namarvar H, Shahidi A (2004) Cardiac arrhythmias predictive detection methods with wavelet-svd analysis and support vector machines. In: Engineering in Medicine and Biology Society, 2004. IEMBS'04. 26th Annual international conference of the IEEE, vol 1. IEEE, New York, pp 365–368
26. Nanthakumar K, Walcott G, Melnick S, Rogers J, Kay M, Smith W, Ideker R, Holman W (2004) Epicardial organization of human ventricular fibrillation. Heart Rhythm 1(1):14–23
27. Narayan SM, Krummen DE, Shivkumar K, Clopton P, Rappel WJ, Miller JM (2012) Treatment of atrial fibrillation by the ablation of localized sources. J Am Coll Cardiol 60(7):628–636
28. Omar M, Solouma N, Kadah Y (2006) Morphological characterization of ecg signal abnormalities: a new approach. In: Proceedings of Cairo international biomedical engineering conference, pp 1–5
29. Ozkurt N, Savaci F (2005) Determination of wavelet ridges of nonstationary signals by singular value decomposition. Circuits Syst II Express Briefs IEEE Trans 52(8):480–485. doi:10.1109/TCSII.2005.849041
30. Potse M, Essebag V (2009) Guidance for catheter ablation of ventricular arrhythmia. Med Biol Eng Comput 47(3):241–243
31. Povinelli RJ, Roberts FM, Ropella KM, Johnson MT (2002) Are nonlinear ventricular arrhythmia characteristics lost, as signal duration decreases? In: Proceedings. Computers in Cardiology, Memphis, TN, pp 221–224
32. Roberts F, Povinelli R, Ropella K (2001) Identification of ecg arrhythmias using phase space reconstruction. Principles of data mining and knowledge discovery, pp 411–423
33. Rocha T, Paredes S, de Carvalho P, Henriques J, Antunes M (2008) Phase space reconstruction approach for ventricular arrhythmias characterization. In: Engineering in Medicine and Biology Society, 2008. EMBS 2008. 30th Annual international conference of the IEEE. IEEE, New York, pp 5470–5473
34. Ropella K, Baerman J, Sahakian A, Swiryn S (1990) Differentiation of ventricular tachyarrhythmias. Circulation 82(6):2035–2043
35. Samie F, Berenfeld O, Anumonwo J, Mironov S, Udassi S, Beaumont J, Taffet S, Pertsov A, Jalife J (2001) Rectification of the background potassium current: a determinant of rotor dynamics in ventricular fibrillation. Circ Res 89(12):1216
36. Samie F, Jalife J (2001) Mechanisms underlying ventricular tachycardia and its transition to ventricular fibrillation in the structurally normal heart. Cardiovasc Res 50(2):242
37. Sierra G, de Jesu's Go'mez M, Le Guyader P, Trelles F, Cardinal R, Savard P, Nadeau R (1998) Discrimination between monomorphic and polymorphic ventricular tachycardia using cycle length variability measured by wavelet transform analysis. J Electrocardiol 31(3):245–255
38. SPSS Inc (1990) SPSS advanced statistics user's guide. In: User manual, SPSS Inc., Chicago, IL
39. Strang G (2003) Introduction to linear algebra. Wellesley Cambridge Press, Wellesley
40. Strohmenger H, Lindner K, Brown C (1997) Analysis of the ventricular fibrillation ECG signal amplitude and frequency parameters as predictors of countershock success in humans. Chest 111(3):584
41. Ten Tusscher K, Mourad A, Nash M, Clayton R, Bradley C, Paterson D, Hren R, Hayward M, Panfilov A, Taggart P (2009) Organization of ventricular fibrillation in the human heart: experiments and models. Exp Physiol 94(5):553
42. Thomas S, Thiagalingam A, Wallace E, Kovoor P, Ross D (2005) Organization of myocardial activation during ventricular fibrillation after myocardial infarction. Circulation 112(2):157–163
43. Tsipouras M, Fotiadis D, Sideris D (2002) Arrhythmia classification using the RR-interval duration signal. In: Computers in cardiology. IEEE, New York, pp 485–488
44. Umapathy K, Krishnan S, Masse S, Hu X, Dorian P, Nanthakumar K (2009) Optimizing cardiac resuscitation outcomes using wavelet analysis. In: International conference of the IEEE engineering in medicine and biology society, vol 1, pp 6761–6764
45. Venkatachalam V, Aravena J (1999) Nonstationary signal classification using pseudo power signatures: the matrix svd approach. Circuits and systems II: analog and digital signal processing. IEEE Trans 46(12):1497–1505. doi:10.1109/82.809535
46. Wall M, Rechtsteiner A, Rocha L (2003) Singular value decomposition and principal component analysis. In: A practical approach to microarray data analysis, pp 91–109
47. Wathen M, DeGroot P, Sweeney M, Stark A, Otterness M, Adkisson W, Canby R, Khalighi K, Machado C, Rubenstein D et al (2004) Prospective randomized multicenter trial of empirical antitachycardia pacing versus shocks for spontaneous rapid ventricular tachycardia in patients with implantable cardioverter-defibrillators. Circulation 110(17):2591–2596
48. Wathen M, Sweeney M, DeGroot P, Stark A, Koehler J, Chisner M, Machado C, Adkisson W (2001) Shock reduction using antitachycardia pacing for spontaneous rapid ventricular tachycardia in patients with coronary artery disease. Circulation 104(7):796–801
49. Watson J, Addison P, Clegg G, Holzer M, Sterz F, Robertson C (2000) A novel wavelet transform based analysis reveals hidden structure in ventricular fibrillation. Resuscitation 43(2):121–127
50. Wilkoff B, Kuhlkamp V, Volosin K, Ellenbogen K, Waldecker B, Kacet S, Gillberg J, DeSouza C (2001) Critical analysis of dual-chamber implantable cardioverter-defibrillator arrhythmia detection: results and technical considerations. Circulation 103(3):381